Journal of Solid State Chemistry **155,** 124–128 (2000)
doi:10.1006/jssc.2000.8912, available online at http://www.idealibrary.com on IDEAL®

Electronic Band Structure Study of $A_2Mo_9S_{11}$ (A=K, Rb) and $K_{1.8}Mo_9S_{11}$

H.-J. Koo and M.-H. Whangbo

Department of Chemistry, North Carolina State University, Raleigh, North Carolina 27695-8204

S. Picard and S. Jobic

Laboratoire de Chimie des Solides, Institut des Matériaux Jean Rouxel, 2 rue de la Houssinière, B. P. 32229, 44322 Nantes Cedex 03, France

and

M. Potel and P. Gougeon

Laboratoire de Chimie du Solide et Inorganique Moléculaire, Université de Rennes 1, UMR 6511, 35042 Rennes Cedex, France

Received June 5, 2000; in revised form July 25, 2000; accepted August 2, 2000

DEDICATED TO PROFESSOR J. M. HONIG

The electronic band structures of $A_2Mo_9S_{11}$ (A=K, Rb) and $K_{1.8}Mo_9S_{11}$ are examined by extended Hückel tight binding calculations. $K_2Mo_9S_{11}$ and $K_{1.8}Mo_9S_{11}$ are metallic and exhibit resistivity anomalies below ~115 and ~80 K, respectively. The origin of these anomalies is explained in terms of their Fermi surfaces. Our study indicates that the resistivity anomalies of these compounds are caused by the partial nesting of their two-dimensional Fermi surfaces and that both $K_2Mo_9S_{11}$ and $Rb_2Mo_9S_{11}$ should exhibit a charge density wave phenomenon.

1. INTRODUCTION

A number of molybdenum chalcogenides contain Mo_{3n} clusters (n = 2–8, 10, 12) in which the Mo_{3n} clusters for $n > 2$ result from the uniaxial trans-face sharing of Mo_6 octahedra (1–12). Recently Picard *et al.* reported that the bioctahedral Mo_9 cluster compounds $K_2Mo_9S_{11}$ and $K_{1.8}Mo_9S_{11}$ exhibit puzzling resistivity anomalies (Figs. 1a and 1b) (13). $K_2Mo_9S_{11}$ is metallic from room temperature to ~115 K, is semiconducting between ~115 and ~50 K, is metallic again below ~50 K, but does not become superconducting. $K_{1.8}Mo_9S_{11}$ is metallic from room temperature to ~80 K, is semiconducting between ~80 and 4.2 K, and becomes superconducting below 4.2 K. The resistivity upturns of these metallic compounds, which occur at relatively high temperatures (~115 and ~80 K for $K_2Mo_9S_{11}$ and $K_{1.8}Mo_9S_{11}$, respectively), may arise from a charge density wave instability. If this is correct, the Fermi surfaces of these compounds should be partially nested (14). Furthermore the extent of partial nesting should be higher for $K_2Mo_9S_{11}$ than for $K_{1.8}Mo_9S_{11}$, because the resistivity upturn occurs at a higher temperature for $K_2Mo_9S_{11}$ and because the extent of the resistivity upturn is larger for $K_2Mo_9S_{11}$. $Rb_2Mo_9S_{11}$ is isostructural and isoelectronic with $K_2Mo_9S_{11}$, but its transport properties have not been measured yet. Thus it would be interesting to see if $Rb_2Mo_9S_{11}$ and $K_2Mo_9S_{11}$ are similar in transport properties. In the present work we calculate the Fermi surfaces of $A_2Mo_9S_{11}$ (A = K, Rb) and $K_{1.8}Mo_9S_{11}$ based on the extended Hückel tight binding (EHTB) method (15, 16). The atomic parameters used for our EHTB calculations are summarized in Table 1.

2. CRYSTAL STRUCTURE

To understand the electronic band structures of $A_2Mo_9S_{11}$ (A = Rb, K) and $K_{1.8}Mo_9S_{11}$ discussed in the next section, it is necessary to describe their crystal structures. These compounds are made up of Mo_9S_{11} clusters (Fig. 2a). Each Mo_9S_{11} cluster has a bioctahedral Mo_9 unit obtained by stacking three Mo_3 triangles. To a first approximation, every edge of each Mo_3 triangle is capped by an S atom to form a planar Mo_3S_3 unit. Thus stacking of three Mo_3S_3 units leads to a Mo_9S_9 cluster. When the outer two Mo_3 triangles of a Mo_9S_9 cluster are each face-capped by S atoms, a Mo_9S_{11} cluster results. The Mo and S atoms of the outer two Mo_3S_3 units of a Mo_9S_{11} cluster are used to form two Mo(2)–S(2) bonds between every two adjacent Mo_9S_{11} clusters (Fig. 2b). Thus each Mo_9S_{11} cluster is connected to three Mo_9S_{11} clusters using the topmost Mo_3S_3 unit and also to three Mo_9S_{11} clusters using

0022-4596/00 $35.00

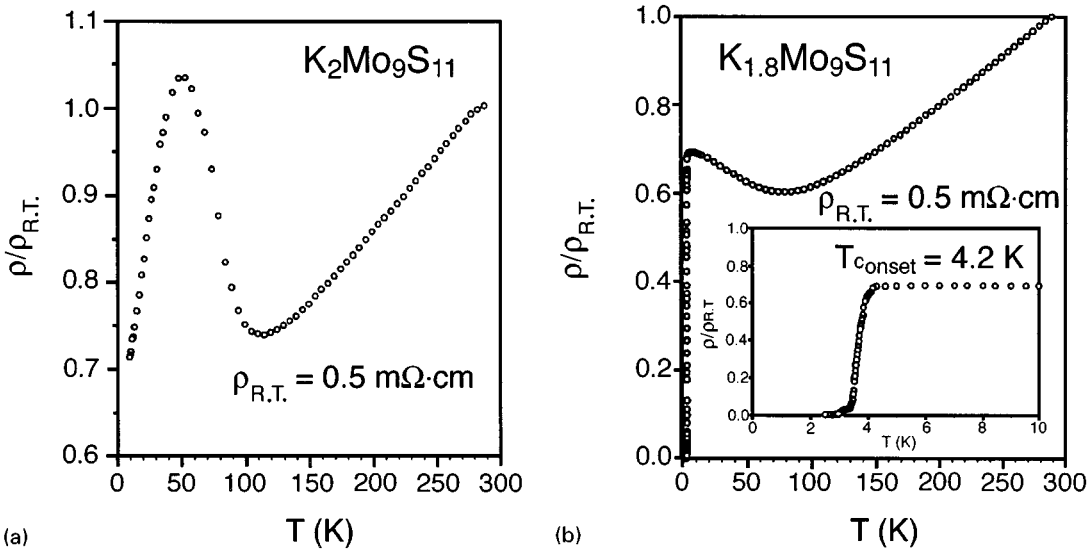

FIG. 1. Electrical resistivities of (a) $K_2Mo_9S_{11}$ and (b) $K_{1.8}Mo_9S_{11}$ as a function of temperature (taken from Ref. 13).

the bottommost Mo_3S_3 unit. Consequently, the $A_2Mo_9S_{11}$ (A = Rb, K) and $K_{1.8}Mo_9S_{11}$ phases consist of pseudohexagonal layers of Mo_9S_{11} clusters parallel to the *ab*-plane (Fig. 2c).

3. DENSITY OF STATES AND FERMI SURFACE

The plots of the density of states (DOS) calculated for the *d*-block bands of $K_2Mo_9S_{11}$, $Rb_2Mo_9S_{11}$, and $K_{1.8}Mo_9S_{11}$ are presented in Figs. 3a–3c, respectively, where the arrows indicate the Fermi levels. For simplicity, only the bottom portion of the *d*-block bands is shown for each compound. The plots of the projected DOS (PDOS) calculated for the *d* orbitals of the Mo(1) and Mo(2) atoms are also shown. In general, the DOS and PDOS plots of the three compounds are very similar and hence the difference in the electrical resistivities of $K_2Mo_9S_{11}$ and $K_{1.8}Mo_9S_{11}$ cannot be clearly distinguished in terms of their DOS and PDOS plots.

The Fermi surfaces calculated for $K_2Mo_9S_{11}$, $Rb_2Mo_9S_{11}$, and $K_{1.8}Mo_9S_{11}$ are shown in Figs. 4–6, respectively. Both $K_2Mo_9S_{11}$ and $K_{1.8}Mo_9S_{11}$ have two-dimensional (2D) Fermi surfaces, which occur in the form of warped cylinders running along the Γ–Z direction, and have three-dimensional (3D) Fermi surfaces as well. However, $K_2Mo_9S_{11}$ has more 2D Fermi surfaces than $K_{1.8}Mo_9S_{11}$ (five versus two, see Figs. 4a and 6a along the Γ–Y direction) and has less 3D Fermi surfaces than $K_{1.8}Mo_9S_{11}$. Consequently, $K_2Mo_9S_{11}$ has a 2D character stronger than that of $K_{1.8}Mo_9S_{11}$. In addition, the 2D Fermi surfaces of $K_2Mo_9S_{11}$ are generally less warped than those of $K_{1.8}Mo_9S_{11}$. Thus the extent of partial nesting is larger for $K_2Mo_9S_{11}$ than for $K_{1.8}Mo_9S_{11}$. Therefore, in terms of charge density wave instability, it is easy to understand why the resistivity upturn is stronger and occurs at a higher temperature for $K_2Mo_9S_{11}$ than for $K_{1.8}Mo_9S_{11}$. $Rb_2Mo_9S_{11}$ consists of only 2D Fermi surfaces (Fig. 5) and is expected to have a charge density wave instability at a higher temperature than does $K_2Mo_9S_{11}$.

TABLE 1
Exponent (ζ_i and $\zeta_{i'}$) and Valence Shell Ionization Potentials (H_{ii}) of Slater-Type Orbitals (χ_i) Used for Extended Hückel Molecular Orbital Calculations[a]

Atom	χ_i	H_{ii} (eV)	ζ_i	c_1[b]	$\zeta_{i'}$	c_2[b]
Mo	5*s*	− 8.34	1.960	1.0000		
Mo	5*p*	− 5.24	1.900	1.0000		
Mo	4*d*	− 10.5	4.540	0.6097	1.900	0.6097
S	3*s*	− 20.0	2.122	1.0000		
S	3*p*	− 13.3	1.827	1.0000		

[a] H_{ii}s are the diagonal matrix elements $\langle\chi_i|H^{eff}|\chi_i\rangle$, where H^{eff} is the effective Hamiltonian. In our calculations of the off-diagonal matrix elements $H_{ij} = \langle\chi_i|H^{eff}|\chi_j\rangle$, the weighted formula was used (see Ref. 17).

[b] Contraction coefficients used in the double-zeta Slater-type orbital.

4. CONCLUDING REMARKS

Our calculations show that $K_2Mo_9S_{11}$ and $K_{1.8}Mo_9S_{11}$ have both 2D and 3D Fermi surfaces. $K_2Mo_9S_{11}$ has more 2D and less 3D Fermi surfaces than $K_{1.8}Mo_9S_{11}$, and the 2D Fermi surfaces of $K_2Mo_9S_{11}$ are generally less warped than those of $K_{1.8}Mo_9S_{11}$. Although 3D in crystal structure, $K_2Mo_9S_{11}$ exhibits quite a strong 2D character in electronic structure. These explain, from the viewpoint of

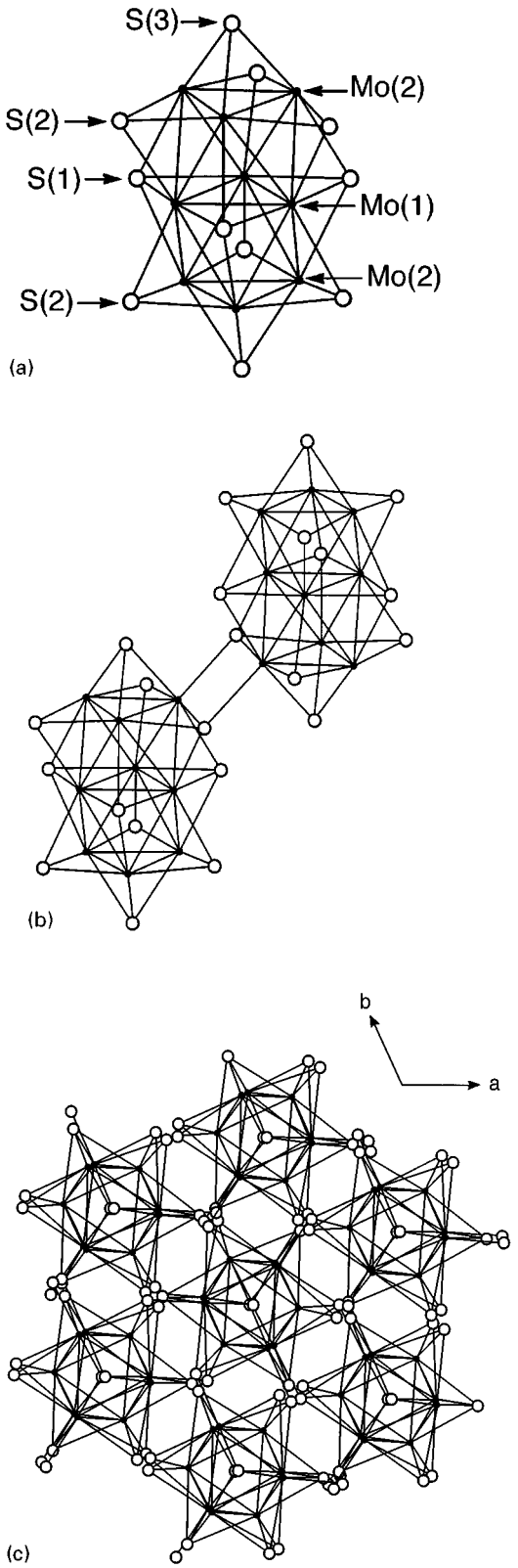

FIG. 2. (a) Perspective view of a Mo_9S_{11} cluster. (b) Perspective view of two adjacent Mo_9S_{11} clusters joined by two intercluster Mo(2)–S(2) bonds. (c) Projection view of layers of Mo_9S_{11} clusters along the c direction.

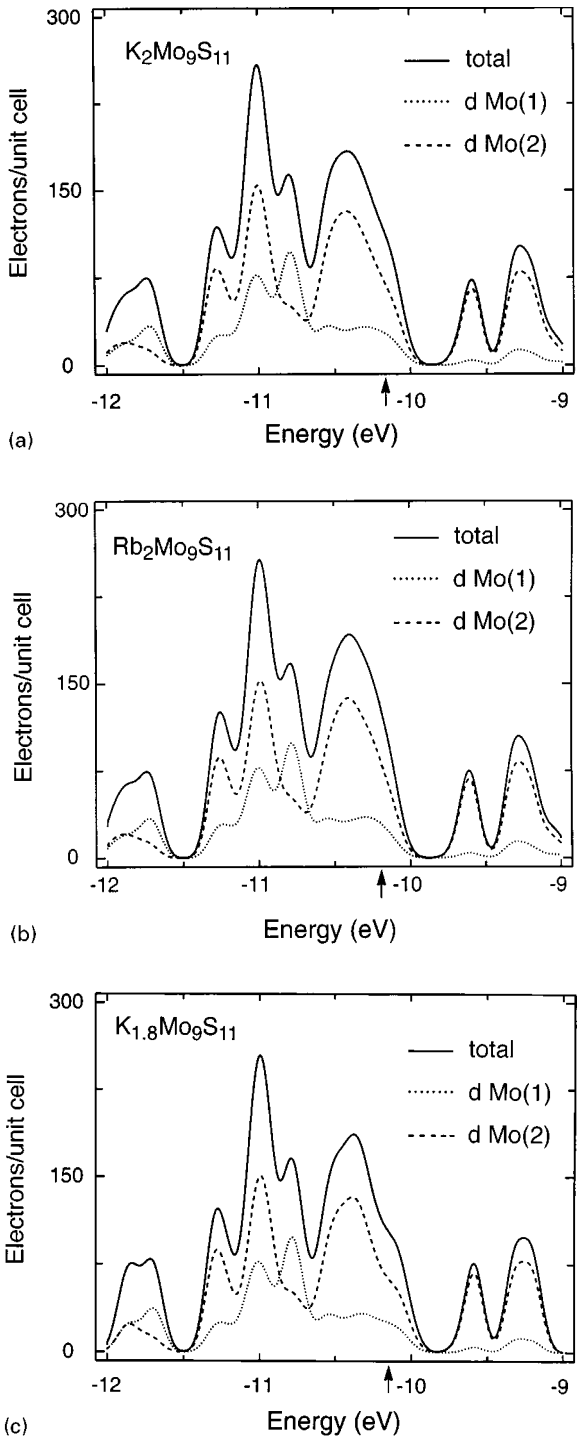

FIG. 3. DOS and PDOS plots calculated for (a) $K_2Mo_9S_{11}$, (b) $Rb_2Mo_9S_{11}$, and (c) $K_{1.8}Mo_9S_{11}$. The arrows indicate the Fermi levels.

charge density wave instability, why the resistivity upturn is stronger and occurs at a higher temperature for $K_2Mo_9S_{11}$ than for $K_{1.8}Mo_9S_{11}$. Our calculations suggest that charge density wave instability is stronger for $Rb_2Mo_9S_{11}$ than for

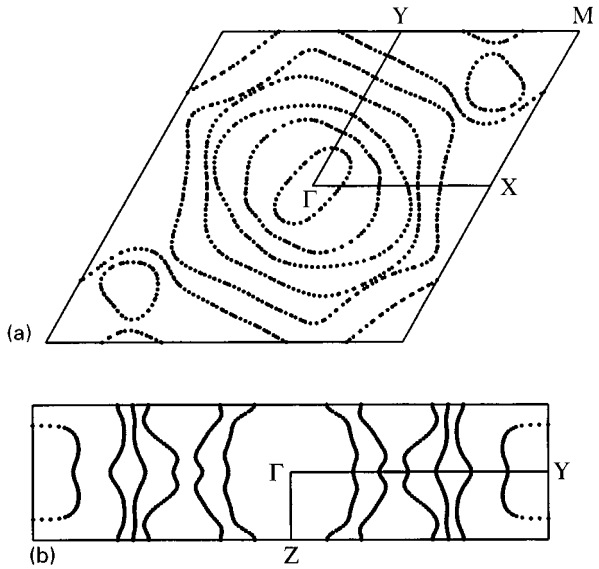

FIG. 4. Cross-section views of the Fermi surfaces calculated for $K_2Mo_9S_{11}$ on (a) the a^*b^* plane at the c^* height of 0 and (b) the b^*c^* plane at the a^* height of 0.

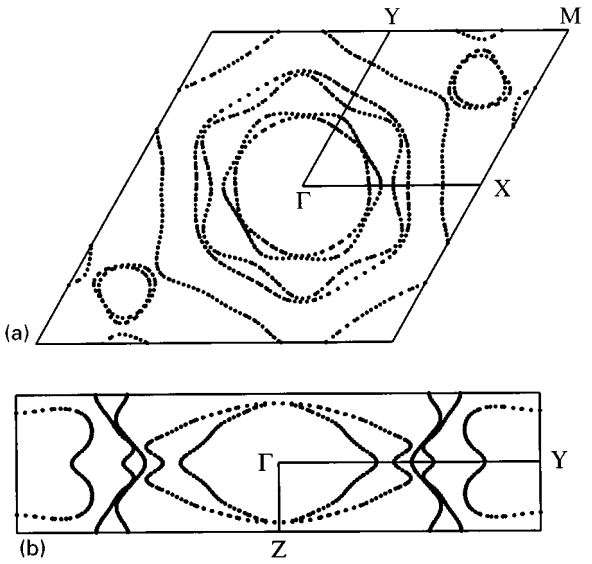

FIG. 6. Cross-section views of the Fermi surfaces calculated for $K_{1.8}Mo_9S_{11}$ on (a) the a^*b^* plane at the c^* height of 0 and (b) the b^*c^* plane at the a^* height of 0.

$K_2Mo_9S_{11}$. It would be interesting to test the occurrence of a charge density wave phenomenon in $K_2Mo_9S_{11}$ and $Rb_2Mo_9S_{11}$ by performing electron or diffuse X-ray scattering experiments.

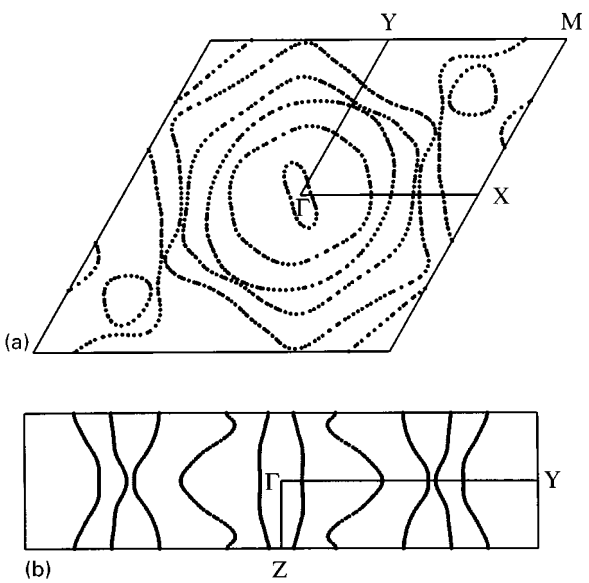

FIG. 5. Cross-section views of the Fermi surfaces calculated for $Rb_2Mo_9S_{11}$ on (a) the a^*b^* plane at the c^* height of 0 and (b) the b^*c^* plane at the a^* height of 0.

ACKNOWLEDGMENTS

The work at North Carolina State University was supported by the Office of Basic Energy Sciences, Division of Materials Sciences, U.S. Department of Energy, under Grant DE-FG05-86ER45259.

REFERENCES

1. R. Chevrel and M. Sergent, *in* "Superconductivity in Ternary Compounds" (O. Fischer and B. M. Maple, Eds.), Part I. Springer-Verlag, New York, 1982.
2. O. Fischer, *Appl. Phys.* **16,** 1 (1978).
3. B. M. Maple and O. Fischer, *in* "Superconducting in Ternary Compounds" (O. Fisher and B. M. Maple, Eds.), Parts I and II. Springer-Verlag, New York, 1982.
4. P. Gougeon, J. Padiou, J.-Y. Le Marouille, and M. Sergent, *J. Solid State Chem.* **51,** 226 (1984).
5. P. Gougeon, M. Potel, J. Padiou, and M. Sergent, *Mater. Res. Bull.* **22,** 1087 (1987).
6. R. Gautier, S. Picard, P. Gougeon, and M. Potel, *Mater. Res. Bull.* **34,** 93 (1999).
7. P. Gougeon, M. Potel, and M. Sergent, *Acta Crystallogr. C* **45,** 182 (1989).
8. P. Gougeon, M. Potel, and M. Sergent, *Acta Crystallogr. C* **45,** 1413 (1989).
9. P. Gougeon, M. Potel, J. Padiou, and M. Sergent, *Mater. Res. Bull.* **23,** 453 (1988).
10. S. Picard, P. Gougeon, and M. Potel, *Acta Crystallogr. C* **53,** 1519 (1997).
11. P. Gougeon, Thesis, Université de Rennes I, 1984.
12. S. Picard, P. Gougeon, and M. Potel, *Angew. Chem. Int. Ed.* **38,** 2034 (1999).
13. S. Picard, J.-F. Halet, P. Gougeon, and M. Potel, *Inorg. Chem.* **38,** 4422 (1999).
14. E. Canadell and M.-H. Whangbo, *Chem. Rev.* **91,** 965 (1991).

15. M.-H. Whangbo and R. Hoffmann, *J. Am. Chem. Soc*. **100,** 6093 (1978).
16. Our calculations were carried out by employing the "CAESAR" program package. (J. Ren, W. Liang, and M.-H. Whangbo, "Crystal and Electronic Structure Analysis Using CAESAR." 1998. This book can be downloaded free of charge from the web site http://www.PrimeC.com/.)
17. J. Ammeter, H.-B. Bürgi, J. Thibeault, and R. Hoffmann, *J. Am. Chem. Soc*. **100,** 3686 (1978).